Organic Interfacial Tailoring of Styrene Butadiene Rubber–Clay Nanocomposites Prepared by Latex Compounding Method

Qing-Xiu Jia,[1] You-Ping Wu,[2] Yi-Qing Wang,[2] Ming Lu,[1] Jian Yang,[1] Li-Qun Zhang[1,2]

[1]*The Key Laboratory of Beijing City on Preparation and Processing of Novel Polymer Materials, Beijing 100029, China*
[2]*The Key Laboratory for Nanomaterials, Ministry of Education, Beijing University of Chemical Technology, Beijing 100029, China*

Received 14 July 2006; accepted 6 August 2006
DOI 10.1002/app.25299
Published online in Wiley InterScience (www.interscience.wiley.com).

ABSTRACT: The styrene butadiene rubber (SBR)–clay nanocompounds were prepared by the latex compounding method, and then hexadecyl trimethyl ammonium bromide (C16) and 3-aminopropyl triethoxy silane (KH550) were added into these nanocompounds on a two-roll mill to prepare nanocomposites with strong interfacial interaction. The structure and properties of SBR–clay nanocomposites were carefully studied by X-ray diffraction (XRD) studies, transmission electron microscopy (TEM), Rubber Process Analyzer (RPA), and mechanical testing. Compared with unmodified nanocomposites, the dispersion structure of modified SBR–clay nanocomposites is better with part rubber-intercalated or part modifier-intercalated structure. The tensile strength and the modulus at 300% elongation of modified SBR–clay nanocomposites are higher than three times of those of unmodified nanocomposites, respectively. © 2006 Wiley Periodicals, Inc. J Appl Polym Sci 103: 1826–1833, 2007

Key words: latex compounding method; rubber; clay; nanocomposites; modification

INTRODUCTION

In the past decade polymer–clay nanocomposites are of great interest, both in academic researches and industrial applications, because they often exhibit remarkable improvement in materials properties when compared with virgin polymer or conventional micro- and macrocomposites.[1–6] Clay minerals are composed of silicate layers about 1 nm thick and several hundreds of nanometers in the lateral dimension.[7] In the aforementioned nanocomposites, the clay was dispersed in the polymer matrix at the nanoscale.

As a kind of inorganic fillers, clay is hydrophilic in nature, and this property makes it very difficult to disperse into a polymer matrix. Generally, the hydrophilic pristine-layered silicates would be intercalated using organic modifiers via cation exchange reaction.[8,9] This is the most common way to improve the affinity of inorganic-layered silicates with organic polymers. The most popular modifiers are organic quarternized ammonium or phosphonium, preferably with long alkyl chains, for instance, hexadecyl trimethyl ammonium bromide (C16), octadecyl trimethyl ammonium chloride, dodecyl trimethyl ammonium bromide, and so forth. Silane coupling agents such as 3-aminopropyl triethoxy silane (KH550) was also used to modify clay.[10] Currently, melt blending organically modified clay with plastic polymer to make clay–polymer nanocomposite mainly with intercalated structure has become a popular way since it well facilitate the polymer processing techniques. Now the organically modified clay fines are used as fillers in most polymer–clay nanocomposites.

Clay and clay minerals such as montmorillonite, saponite, hectorite, etc., have been used as rubber fillers for many years, to save rubber consumption, reduce cost, and improve the processing properties of rubbers.[11–13] However, it was reported that the incorporation of layered silicate to rubber in nanoscale could bring the significant improvement in the properties of materials.[14,15] Nowadays rubber–clay nanocomposites have been developed by various methods, including *in situ* polymerization intercalation,[16] solution intercalation,[17] melt intercalation,[18] and cocoagulating rubber latex and clay aqueous suspension (namely LCM).[14,15] Among them, the approach of cocoagulating rubber latex and clay aqueous suspension, where pristine clay is directly employed, is promising for industrialization because of the low cost of pristine clay, simplicity of preparation process, and superior performance/cost ratio. In

Correspondence to: L. Q. Zhang (zhanglq@mail.buct.edu.cn or 2004080057@grad.buct.edu.cn).

Contract grant sponsor: Beijing New Star Plan Project; contract grant number: H010410010112.
Contract grant sponsor: National Tenth Five-year Program; contract grant number: 2001BA310A12.

TABLE I
Formulation of the Mixes

Ingredients	Contents (phr[a])
SBR	100
Clay	10
Hexadecyl trimethyl ammonium bromide (or 3-aminopropyl triethoxy silane)	5 (or 4)
Zinc oxide	5.0
Stearic acid	2.0
Diphenyl guanidine	0.5
Dibenzothiazode disulfide	0.5
Tetramethyl thiuram disulfide	0.2
N-Isopropyl-*N*′-phenyl-*p*-phenylene diamine	1.0
Sulfur	2.0

[a] phr is the abbreviation of weight parts per 100 weight parts rubber.

general, polymer–clay nanocomposites are of two different types, namely intercalated structure and exfoliated structure. The structure of rubber–clay nanocomposites prepared by LCM is different from intercalated and exfoliated clay nanocomposites, in which the rubber molecules ''separated'' the clay particles into either individual layers or just silicate layer aggregates of nanometer thickness without the intercalation of rubber molecules into clay galleries. Such a structure was found to result from the competition between separation of rubber latex particles and reaggregation of single silicate layers during the cocoagulating process.[19] It was also reported that the flocculant cations, for instance H^+, Ca^{2+}, and RNH_3^+, could intercalate into silicate layers. At the same time, the interfacial compatibility would be poor without special interfacial modification. In our previous work,[20] *N*-allyl dimethyl octadecanamine chloride was introduced into clay aqueous suspension to *in situ* organically modify clay before rubber latex was added in, to improve the interfacial interaction. As a result, the tensile strength of styrene butadiene rubber (SBR)–clay (100/10) nanocomposites increased from 4.3 to 18.7 MPa. It was also found that in that way there was a competition of intercalation between the modifier cations and the flocculant cations, and the amount of rubber-intercalated structure or modifier-intercalated structure strongly depended on the result of the above competition.

In this article, a novel way to increase the interfacial interaction between pristine clay and rubber was developed. First SBR–clay nanocomposite was prepared by LCM with diluted sulfuric acid solution and calcium chloride aqueous solution as flocculating agents. And then, C16 or KH550 was directly introduced into the SBR–clay nanocompounds on a two-roll mill with other ingredients to prepare SBR–clay nanocomposites. Compared with *in situ* modification in suspension, this method seems to be simpler and more feasible. The results acquired can provide some reference to the preparation of high-performance rubber–clay nanocomposites with good interfacial interaction.

EXPERIMENTAL

Materials

SBR latex (St 23%, solid content 22.4%) was from Jilin Petrochemical Co., China; the clay (Na^+-montmorillonite), with a cationic exchange capacity (CEC) of 78 mequiv./100 g, was supplied by Liufangzi Clay Factory, Jilin, China. Hexadecyl trimethyl ammonium bromide (C16) was provided by Beijing Chemical Reagents Co., Beijing, China. 3-Aminopropyl triethoxy silane (KH550) was purchased from Nanjing Shuguang Chemical Group Co., Jiangsu, China. Other ingredients, such as zinc oxide, stearic acid, sulfur, and diluted sulfuric acid solution were of commercial grade.

Preparation of SBR–clay nanocomposites

About 2% aqueous suspension of clay and the SBR latex were mixed and vigorously stirred for a given period of time. After that the mixture was cocoagulated in the electrolyte solution (1% calcium chloride aqueous solution or 2% sulfuric acid solution), washed in water, and dried in an oven at 50°C for 20 h, and then the SBR–clay nanocompound was obtained. Here it must be made clear that the nanocompounds are referred to as uncured ones, and the nanocomposites as cured ones in this article.

The modifier (C16 or KH550), the vulcanizing ingredients, and other additives were mixed into the nanocompound on a 6-in. two-roll mill, according to the recipe listed in Table I. Then the compound was vulcanized in a standard mold with about 15 MPa pressure at 150°C. The vulcanizates are referred to as SBR–clay nanocomposites. Table II gives the sample designations of all the SBR–clay nanocomposites in this article.

TABLE II
Designation of the SBR–Clay (100/10) Nanocomposites

Flocculant ions	H^+	Ca^{2+}	H^+	H^+	Ca^{2+}	Ca^{2+}
Modifier	No modifier	No modifier	C16	KH550	C16	KH550
Nanocomposites designation	H	Ca	HC16	HKH550	CaC16	CaKH550

Characterization

Transmission electron microscopy (TEM) images were taken with an H-800 TEM (Hitachi, Japan) at an accelerator voltage of 200 kV.

X-ray diffraction (XRD) measurements were carried out using a diffractometer (D/Max- C, Rigaku, Japan) with CuKα radiation operating at 40 kV and 200 mA, at a scan rate of 1° per minute. Space changing of silicate layers in organically modified SBR–clay nanocomposites was observed in the 2θ range of 0.5° to 10°.

The mechanical behavior of the nanocomposites was characterized by means of tensile tests according to ASTM D412 using a CMT4104 electrical tensile tester (SANS, ShenZhen, China). XY-1 rubber hardness apparatus (4th Chemical Industry Machine Factory, Shanghai) was used to measure the Shore A hardness of the vulcanizates.

Strain sweep experiments were performed using the RPA 2000 Rubber Process Analyzer of Alpha Technologies Co., at a fixed frequency and 60°C. The strain was varied from 1% to 42% at the frequency of 10 Hz for cured compounds (i.e., nanocomposites), and 60°C from 1% to 400% at 1 Hz for the uncured compounds.

RESULTS AND DISCUSSION

XRD analysis

The XRD patterns of SBR–clay nanocomposites prepared by different flocculants and organic modifiers are shown in Figure 1. To investigate the effect of heat and pressure on the structure of clay in the rubber matrix, the uncured and cured modified SBR–clay nanocomposites were carefully studied by XRD.

Figure 1(a) gives the XRD patterns for the H^+-flocculated SBR–clay nanocomposites. On the curve of H-cured nanocomposite, there is one peak at 2θ = 6.29°, corresponding to a basal spacing of 1.43 nm, a little bigger than that of Na^+-MMT, which results from the intercalation of flocculant ions into the clay galleries during the flocculating process. However, on the basis of the experience of studying rubber–clay nanocomposites prepared by LCM for these years, this H^+-intercalated structure is a ''separated'' structure.[19] Although there is no rubber macromolecules intercalation, it is still a nanostructure, which can be proved by the TEM photos in the next part. For the uncured SBR–clay nanocomposite with C16 added on the two-roll mill, there are three peaks, corresponding to basal spacing of 1.43, 2.08, and 4.37 nm, respectively. Obviously the adding of C16 intensively changes the structure of clay in the SBR matrix. Although the H^+-intercalated structure remains, two new structures of C16-intercalated and SBR-intercalated emerge which indicates that C16 can intercalate

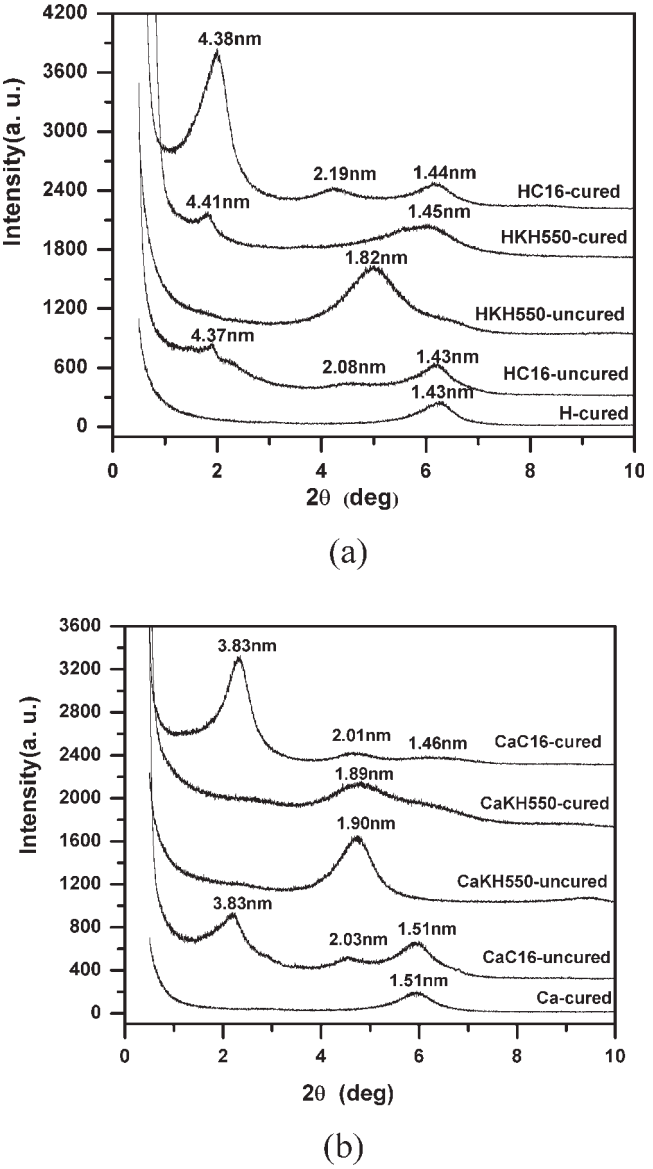

Figure 1 X-ray diffraction spectrum of SBR–clay nanocomposites flocculated by different flocculating agents. (a) H^+-flocculated system; and (b) Ca^{2+}-flocculated system.

into part of silicate layers during general mechanical processing through ion exchange between H^+ and C16. And this C16-intercalation can further induce the intercalation of SBR macromolecules to clay galleries because of the strong shearing force. After vulcanization, similar peaks but with stronger intensity appear for the HC16-cured nanocomposite possibly because of the orientation and reaggregation of clay layers by hot pressure during vulcanization.[21] Compared with C16, KH550 can completely intercalate into the clay galleries during the compounding process, representing a single peak with a 1.82 nm layer spacing on the XRD patterns. Here the XRD peak of H^+-intercalated structure almost disappears. After vulcanization, this singe peak disappears, and as a

result, two new peaks emerge corresponding to layer spacing of 4.41 and 1.45 nm. It can be explained that because of the strong intercalation between H^+ and amine group of KH550, KH550 easily intercalates into the H^+ clay layers. However, on one hand the layer space of KH550 intercalated clay is small, and on the other hand the physical compatibility between KH550 and SBR rubber chains is not good enough, so the rubber intercalation does not evidently happen during mixing. During the curing process, the KH550 with amine group and ethyl hydroxyl group participates in vulcanization and connects with rubber macromolecules by chemical bonding, so the SBR macromolecules are drawn into some clay galleries and result in the small peak of 4.41 nm on the XRD patterns. Because of the same reason, part of KH550 is drawn out from the clay galleries. Thus a new peak with 1.45 nm layer spacing is observed.

In the case of Ca^{2+} as flocculant, similar results can be gained except that the clay layer spacings of all kinds of intercalated structures are different. With bigger size of Ca^{2+}, the layer spacing of Ca^{2+}-intercalated structure is 1.51 nm. But for the uncured and cured CaC16 nanocomposites, the layer spacing of SBR-intercalated structure changes from about 4.40 to 3.83 nm, possibly on account of the strong layer–layer intercalation led by Ca^{2+}. In comparison with Figure 1(a), the biggest difference in Figure 1(b) is the curve of CaKH550-cured nanocomposite, in which only a single peak is observed, weak but very broad, corresponding to the KH550-intercalated structure of 1.9 nm layer spacing. That is still because that the strong layer–layer interaction of clay led by Ca^{2+} makes it very difficult for KH550 to intercalate into clay galleries during the vulcanization process.

TEM characterization

To investigate the effect of modifiers and flocculating agents on the dispersion of clay and interfacial interaction between clay and SBR matrix, the morphologies of a series of SBR–clay nanocomposites were observed with TEM, as shown in Figure 2. The dark lines in the photographs are the intersections of the dispersed silicate layers or layer aggregates. It is worthwhile to note that the dispersion of clay in each photo is good. For unmodified SBR–clay nanocomposite, seen in Figure 2(a,b), the dimensions of the dispersed clay layers are quite fine and their spatial distributions are homogeneous. All the clay layers exist in aggregate form with 10–20 nm thickness. In Figure 2(b), some cavities are observed near the interface between clay layers and rubber matrix, which is caused by the poor interfacial interaction between the pristine clay and SBR. Compared with that of nanocomposite of Ca, the clay layers of nanocomposite of H disperse finer and the interfacial strength seems a little better. When KH550 or C16 is used to modify SBR–clay nanocomposites, the dimension of most dispersed clay layers and the amount of

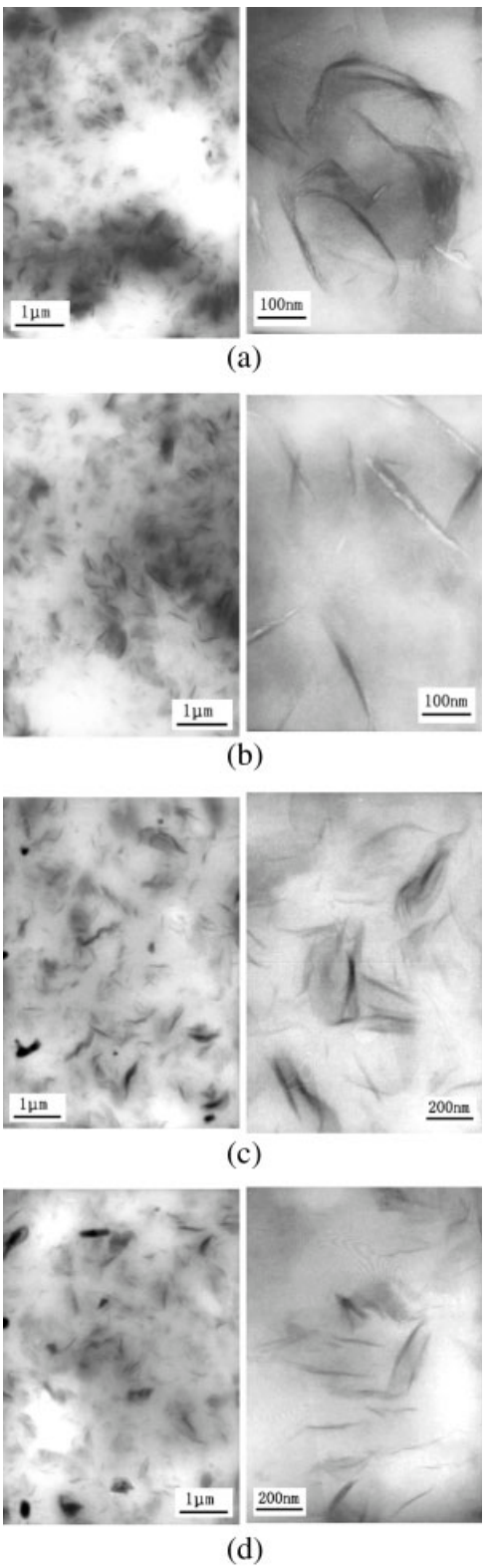

Figure 2 TEM photos of SBR–clay nanocomposite. (a) H; (b) Ca; (c) HKH550; and (d) KC16.

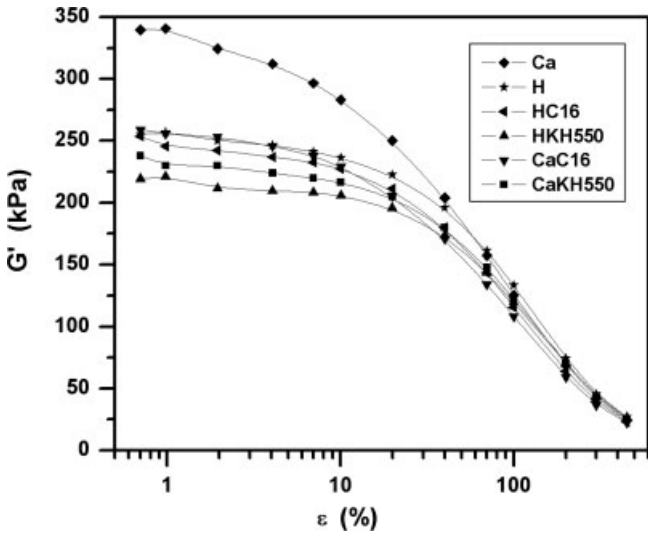

Figure 3 RPA analysis of uncured SBR–clay nanocompounds.

clay aggregates are larger. However, no cavity is found on the interface, and dispersion is homogenous. That not only means that the modifier improves the compatibility of nanodispersed clay and rubber, but also implies that organic modifier assemble some layers or aggregates to form layer aggregates assisted by pressure during vulcanization.[21,22] This implies KH550 and C16 are efficient compatibilizers of clay and SBR. With KH550 modification, in Figure 2(c), the dispersion of clay is more homogeneous. Comparison of these photos initially demonstrates that KH550 is more efficient. All these results are consistent with that from XRD.

Rheology and dynamic properties

The effect of the amplitude-dependence of the dynamic viscoelastic properties of filled rubbers was performed using RPA2000, which can carry out strain and frequency scanning in a board range, showing information on the dispersion of filler particles in the rubber matrix. Figure 3 shows the dependency of the storage modulus (G') of the uncured modified rubber nanocompounds on the strain amplitude, and a highly nonlinear behavior is observed for each one. It is found that the modulus decreases dramatically with increasing the strain amplitude for all the SBR–clay nanocompounds. This can be explained by the Payne effect.[23] The severe decrease in the modulus with increasing deformation ratio is due to the disentanglement of uncured rubber macromolecules, and the breakdown of filler–rubber network constructed by filler–filler interaction and filler–rubber interaction. Another observation is that compared with KH550-modified SBR–clay nanocompounds, C16-modified SBR–clay nanocompounds possess higher moduli. At the same time, the moduli of C16-modified SBR–clay nanocompounds decrease faster when the strain is over 40%. This is probably because that the longer alkyl chains of C16 provide strong entanglements with SBR chains or by themselves, which can be described by the sketch in Figure 4. However, compared with C16, KH550 has lower compatibility with SBR, and thus its effect on helping constructing network is relatively weak. Different from the modified SBR–clay nanocompounds, the reason why the unmodified nanocompounds possess high moduli is that in those nanocompounds, although both the clay–rubber interaction and the compatibility between clay and SBR are weak, filler–filler interaction is very strong because of filler-aggregation.

To investigate the dynamic properties of cured modified SBR–clay nanocomposites, the dynamic storage modulus (G') and mechanical loss factor (tan δ) were also studied. Two zones are found in Figure 5(a). Zone 1 is the modulus–strain pattern under the

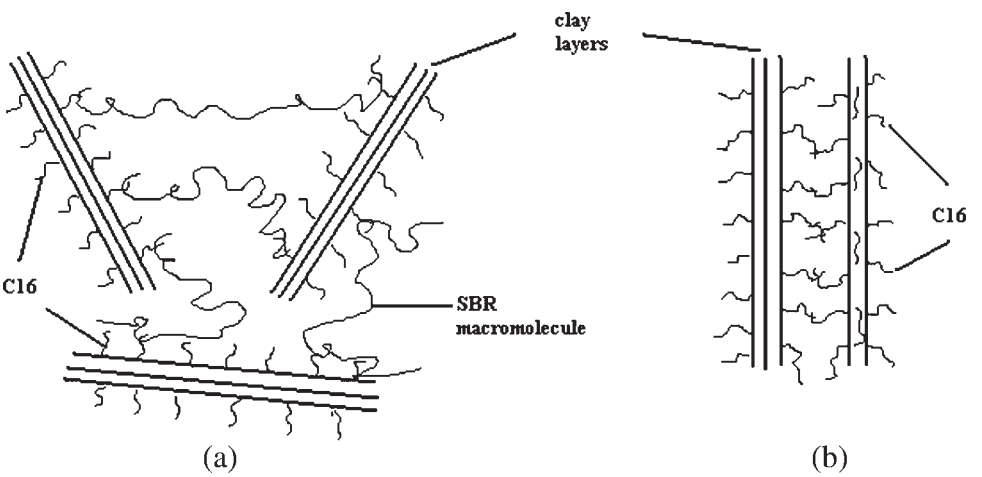

Figure 4 Sketch of physical entanglement between C16 and SBR. (a) Entanglement of SBR with C16 and (b) entanglement of C16 with C16.

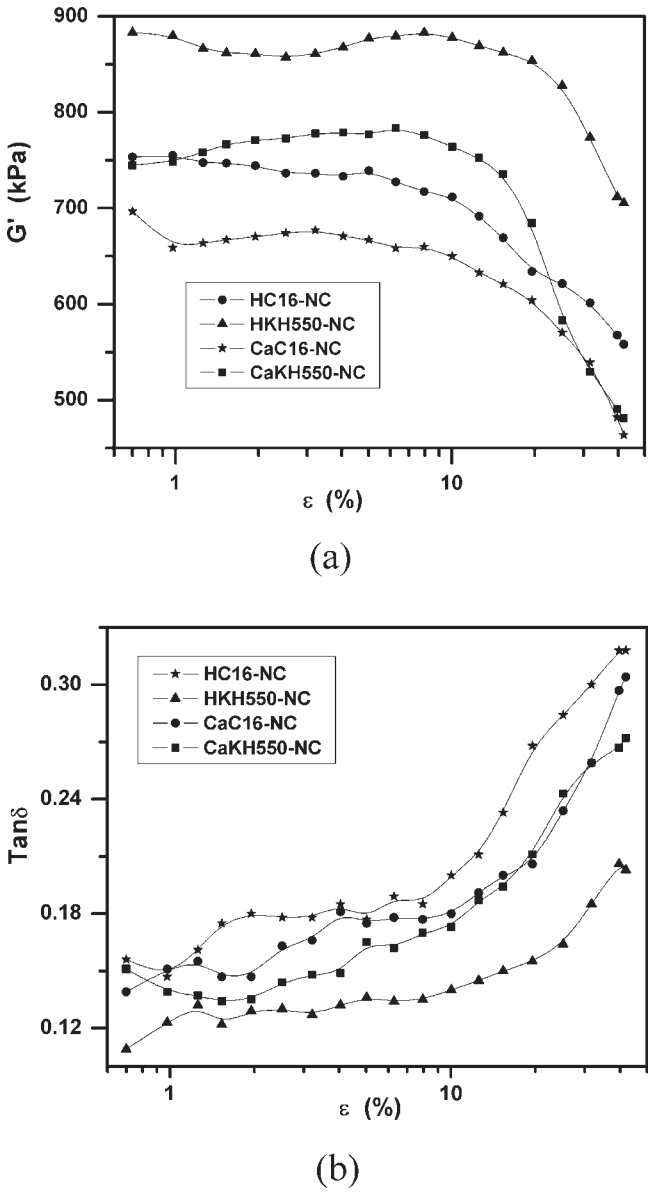

Figure 5 RPA analysis of cured SBR–clay nanocomposites.

100% strain, in which the dynamic shear storage modulus remain constant. When the strain is over 100%, zone 2 is formed, in which the modulus decreases dramatically, similar with what in Figure 3 because of the same reason. On the other hand, it can be found that the order of G' of all the modified SBR–clay nanocomposites is HKH550 > CaKH550 > HC16 > CaC16 and the difference between them is very big, different from that observed in Figure 3. One must pay attention to that compared with Figure 5(a), the order of tan δ of all the modified SBR–clay nanocomposites is reversed in Figure 5(b). Tan δ is dependent on the elasticity of the filled rubber nanocomposites. It is well known that the lower tan δ, the higher the elasticity. High elasticity implies that the material has excellent interface. To understand this, the interfacial interaction among these nanocomposites must be analyzed. At first, we must realize that the layer surface interaction is more important compared with edge interaction since the former is much bigger than the latter in area. C16 physically absorbed on the clay layers, and its long alkyl chains only physically interact with rubber molecules chains even after vulcanization. So the interfacial strength of C16-modified SBR–clay nanocomposites is not strong, which will result in interface sliding during tensile and high hysteresis during dynamic deformation. However, the $—NH_2$ and $—OC_2H_5$ of KH550 can chemically bond with rubber molecules through participating complex curing reaction. Consequently, clay layers will act as the chemical crosslinking points, which further markedly increase the modulus of nanocomposites and remarkably reduce the interfacial hysteresis.

To test this, the effect of modification on curing characteristics is given in Figure 6. Vulcanization is a vital step for rubber product, and the rubber modulus increases dramatically during curing; thus it is used as a monitor to investigate the progress of curing. In Figure 6, for unmodified SBR–clay nanocomposites, the occurrence of vulcanization is delayed. This is caused by the combination of the curing agents with fillers by hydrogen bonding. The combined agents will not crosslink SBR until the combination begins to vanish at the curing temperature. The existence of C16 and KH550 can evidently accelerate the occurrence of vulcanization, as shown in curves for modified nanocomposites. For C16-modified SBR–clay nanocomposites, the maximum torque is reached soon, and remains constant. Different from this, KH550 can obviously shorten the scorch time at first. But as curing progresses, the curing speed becomes slow, and the cure time is protracted. Simultaneously, the torque keeps increasing all the

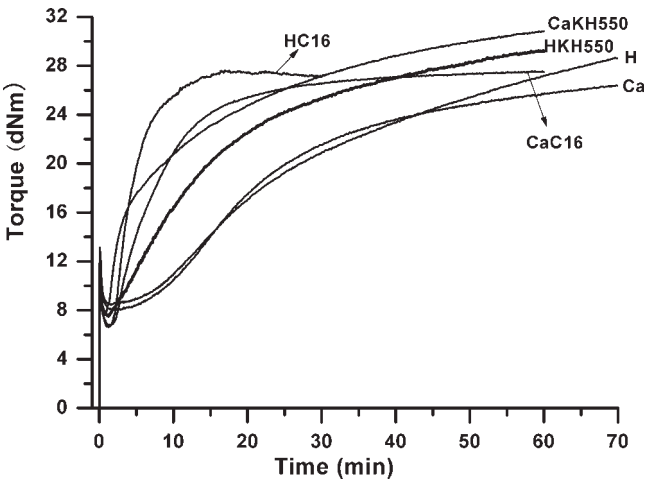

Figure 6 Curing curves of all the SBR–clay (100/10) nanocomposites.

TABLE III
Mechanical Properties of SBR–Clay Nanocomposites

	Mechanical properties						
Nanocomposite	Shore A hardness	Modulus at 100% strain (MPa)	Modulus at 300% strain (MPa)	Tensile strength (MPa)	Elongation at break (%)	Permanent set (%)	Tear strength (kN/m)
Pure SBR	47	0.9	1.1	2.3	632	8	9
H	58	1.4	2.6	4.3	592	24	21
Ca	60	1.2	1.7	4.4	751	36	21
HC16	64	1.9	2.9	9.0	516	28	21
CaC16	62	1.7	2.3	9.4	598	40	20
HKH550	55	1.8	6.8	12.4	504	16	27
CaKH550	57	1.9	5.2	10.1	513	28	26

time. Thus it can be concluded that the existing of KH550 participates in the curing reaction and significantly influences the intercrosslinking structure of SBR–clay nanocomposites.

Mechanical properties of rubber nanocomposites

Table III shows the mechanical properties of pure SBR and unmodified and modified SBR–clay nanocomposites, and the corresponding stress–strain curves are presented in Figure 7. While the tensile strength of pure SBR is measured 2.3 MPa, without organic modification, it is only improved to 4.3 and 4.4 MPa with the addition of 10 phr nanoclay by using H^+ or Ca^{2+} as the flocculating agent, respectively. This improvement is big but not enough to the application requirement. Compared with that of unmodified SBR–clay nanocomposite, no obvious improvement on the tear strength, the stress at 100% or 300% elongation is found, but the tensile strength is improved to about 9.0 MPa for the C16-modified nanocomposites, over 100% improvement, in both systems of H^+ and Ca^{2+} as flocculating agent. With almost the same amount of KH550, the tear strength and the modulus at 100% and 300% of the modified nanocomposites are improved more than 30%, and the tensile strength is also improved to 2.5 times of that of unmodified nanocomposites.

As can be seen from Figure 7, the obvious difference appears even at very small elongation with a value around 40%, and with the increase of elongation, the difference among all the curves becomes more and more distinct. It can be concluded that in the range of median to large strain (e.g., 300% elongation), the stress of H^+-flocculated nanocomposites are higher than that of Ca^{2+}-flocculated nanocomposites for each similar system in which the flocculating agent is the only difference; likewise, the stress at 300% elongation of the modified nanocomposites are much higher than that of unmodified counterparts; moreover, the stress at 300% elongation of KH550-modified nanocomposites are higher than that of C16-modified ones in each system using either H^+ or Ca^{2+}. In the following part, the mechanism of reinforcement will be discussed from the point of the interface sliding and the interfacial interaction during the tensile process. It is well known that modulus at very small strain provides very important information.[24] Here the modulus mainly lies on the strength of network, and indicates the filler dispersion and hardness of the vulcanizate. Within 100% elongation, the order of stress of cured nanocomposites is HC16 > CaC16 > CaKH550 > HKH550, which is consistent with the RPA result of uncured SBR–clay nanocompounds and the Shore A hardness of cured SBR–clay nanocomposites. For nanocomposites of H and Ca, the moduli of their uncured nanocompounds are higher than that of modified nanocompounds because of higher filler–filler interaction; however, the stress of their cured nanocomposites are the lowest among all of the SBR–clay nanocomposites because of the worst clay dispersion in the SBR matrix. With the increase of strain, the interface interaction between filler and matrix dominates the increase of stress. In general, when the interfacial interaction between

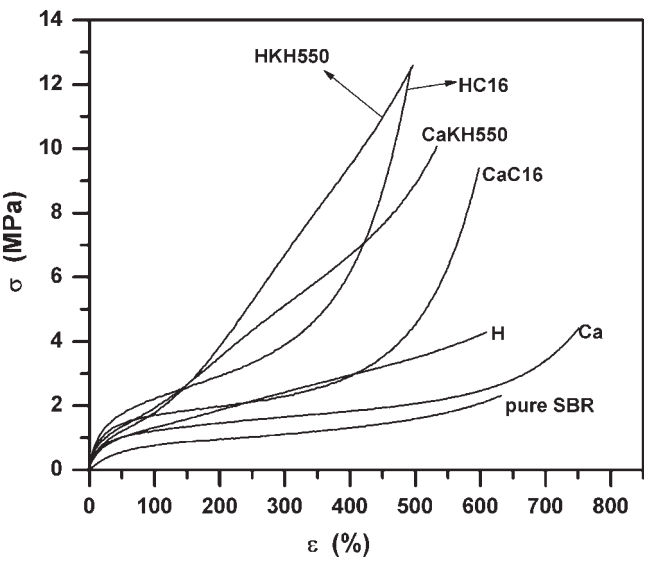

Figure 7 Stress–strain curve of cured SBR–clay nanocomposites.

clay and rubber is chemical linking, the stress at certain strain will be dramatically improved. That is why the curve of KH550-modified SBR–clay nanocomposites is in the highest position when the strain level is over 200% and takes on a steep rise. For C16-modified SBR–clay nanocomposites, the interaction between clay and SBR matrix is physical interaction, i.e., weak Van der Waals forces. However, the interfacial compatibility between clay and SBR is improved because of the existence of C16. During the tensile process, interface sliding between clay layers and SBR matrix occurs, and the rubber macromolecule chains can gradually make an orientation. At the moment, C16 acts as a bridge, which can delay the detachment between clay and rubber molecules. Thus C16 improves the interfacial compatibility and promotes the rise of stress. For the same modifier modified system, the stress at same strain level of H^+-flocculated nanocomposite is always higher than that of the Ca^{2+}-flocculated nanocomposite. The difference of stress–stain curves might attribute to more influence of H^+ on the crosslinking degree of nanocomposites than Ca^{2+}.

CONCLUSIONS

C16 and KH550 were introduced during mixing on a two-roll mill to modify the SBR–clay nanocomposites prepared by the LCM method. With the modification of C16 and KH550, there is part rubber-intercalated structure or part modifier-intercalated structure emerging in the dispersed clay layers, and the dynamic properties of the nanocomposites are remarkably improved. The tensile strength and the modulus at 300% elongation of modified SBR–clay nanocomposites are higher than three times of that of unmodified nanocomposites, respectively.

References

1. Triantafillidis, C. S.; LeBaron, P. C.; Pinnavaia, T. J. Chem Mater 2002, 14, 4088.
2. Shelley, J. S.; Mather, P. T.; DeVries, K. L. Polymer 2001, 42, 5849.
3. Messersmith, P. B.; Giannelis, E. P. Chem Mater 1994, 6, 1719.
4. Manias, E.; Chen, H.; Krishnamoorti, R.; Genzer, J.; Kramer, E. J.; Giannelis, E. P. Macromolecules 2000, 33, 7955.
5. Lim, Y. T.; Park, O. O. Rheol Acta 2001, 40, 220.
6. Joly, S.; Garnaud, G.; Ollitrault, R.; Bokobza, L.; Mark, J. E. Chem Mater 2002, 14, 4202.
7. Alexandre, M.; Dubois, P. Mater Sci Eng R: Rep 2000, 28, 1.
8. Theng, B. K. G. The Chemistry of Clay-Organic Reactions; Wiley: New York, 1974.
9. Ogawa, M.; Kuroda, K. Bull Chem Soc Jpn 1997, 70, 2593.
10. Dai, J. C.; Huang, J. T. Appl Clay Sci 1999, 15, 51.
11. Wu, Y. P.; Jia, Q. X.; Yu, D. S.; Zhang, L. Q. J Appl Polym Sci 2003, 89, 3855.
12. Wang, E.; Pinnavaia, T. J. Chem Mater 1998, 10, 3769.
13. Mehrota, V.; Giannelis, E. P. Mater Res Soc Symp Proc 1990, 171, 39.
14. Wang, Y. Z.; Zhang, L. Q.; Tang, C. H.; Yu, D. S. J Appl Polym Sci 2000, 78, 1879.
15. Zhang, L. Q.; Wang, Y. Z.; Wang, Y. Q.; Sui, Y.; Yu, D. S. JAppl Polym Sci 2000, 78, 1873.
16. Delozier, D. M.; Orwoll, R. A.; Cahoon, J. F.; Johnston, N. J.; Smithm, J. G.; Connell, J. W. Polymer 2002, 43, 813.
17. Jeon, H. S.; Rameshwaram, J. K.; Kim, G.; Weinkauf, D. H. Polymer 2003, 44, 5749.
18. Varghese, S.; Karger-Kocsis, J.; Gatos, K. G. Polymer 2003, 44, 3977.
19. Wu, Y. P.; Wang, Y. Q.; Zhang, H. F.; Wang, Y. Z.; Yu, D. S.; Zhang, L. Q.; Yang, J. Compos Sci Technol 2005, 65, 1195.
20. Jia, Q. X.; Wu, Y. P.; Xu, Y. L.; Mao, H. H.; Zhang, L. Q. Macromol Mater Eng 2006, 291, 218.
21. Liang, Y. R.; Lu, Y. L.; Wu, Y. P.; Ma, Y.; Zhang, L. Q. Macromol Rapid Commun 2005, 26, 926.
22. Liang, Y. R.; Ma, J.; Lu, Y. L.; Wu, Y. P.; Zhang, L. Q.; Mai, Y. W. J Polym Sci B: Polym Phys 2005, 43, 2653.
23. Payne, A. R. In Reinforcement of Elastomers; Kraus, G., Ed.; Wiley Interscience: New York, 1965; Chapter 3, pp 69–123.
24. Meissner, B. Polymer 2000, 41, 7827.